# Haptic Stiffness Perception Using Hand Exoskeletons in Tactile Robotic Telemanipulation

Gabriele Giudici<sup>1,2</sup>, Claudio Coppola<sup>3</sup>, Kaspar Althoefer<sup>1</sup>, Ildar Farkhatdinov<sup>1,4</sup>, Lorenzo Jamone<sup>1,2</sup>

Abstract—Robotic telemanipulation is central in many applications, from healthcare to harsh environments. While visual feedback from cameras can provide valuable information to the human operator, haptic feedback offers insight into certain object properties - such as stiffness - that vision alone cannot provide. However, the use of haptic feedback alone has been largely unexplored. To bridge this gap, we tested ten participants to remotely squeeze soft objects to perceive their stiffness, by teleoperating a dexterous robotic hand using an active hand exoskeleton. Two haptic feedback methods were compared: using only the contact forces measured with the tactile fingertips of the robotic hand, or including a kinematic measure as well (the motion mismatch between the hand exoskeleton and the robotic hand). Our results demonstrate, for the first time, that operators using a hand exoskeleton are indeed capable of discriminating objects of different stiffness relying on haptic feedback alone, with an average accuracy of 75% to identify which object in a pair was most similar to a reference, and 65% to determine which object in a pair was softer. In addition, our findings also suggest that including a kinematic measure in the feedback may enhance discrimination between objects of similar stiffness.

Index Terms—Telerobotics and Teleoperation, Perception for Grasping and Manipulation, Force and Tactile Sensing

# I. Introduction

ROBOTIC teleoperation is a key technology used across diverse real-world applications, from healthcare to harsh environments [1]–[4]. A crucial task in teleoperation is telemanipulation, which involves manipulating objects via the teleoperated robot [5]. Perceiving the physical properties of remote objects is essential for both effective manipulation and information gathering, whether for object recognition or assessing specific attributes, such as determining if manipulated tissue contains a tumor or whether a strawberry is ripe. In bilateral telemanipulation, the user operates a device (leader)

Manuscript received: October 30, 2024; Revised March 21, 2025; Accepted July 16, 2025. This paper was recommended for publication by Editor Angelika Peer upon evaluation of the Associate Editor and Reviewers' comments. This work is partially funded by the UKRI through the EPSRC grants EP/R02572X/1 (NCNR) and EP/V035304/1 (q-Arena). This work involved human subjects in its research. Approval of all ethical and experimental procedures and protocols was granted by the Queen Mary Ethics of Research Committee under Application No. QMERC20.565.DSEECS24-053, and performed in line with the Application of - Enhancing Teleoperation with Exoskeletal Gloves: Leveraging Tactile Sensing for Bilateral Haptic Stiffness Feedback.

<sup>1</sup>ARQ (the Centre for Advanced Robotics @ Queen Mary), School of Engineering and Materials Science, UK (emails: {k.althoefer}@qmul.ac.uk).

<sup>2</sup>Department of Computer Science, University College London, London, WC1E 6BT, UK. (emails: {g.giudici,l.jamone}@ucl.ac.uk).

<sup>3</sup> Humanoid. email: ccop@thehumanoid.ai

<sup>4</sup>School of Biomedical Engineering and Imaging Sciences, King's College London, London, UK.

Digital Object Identifier (DOI): see top of this page.

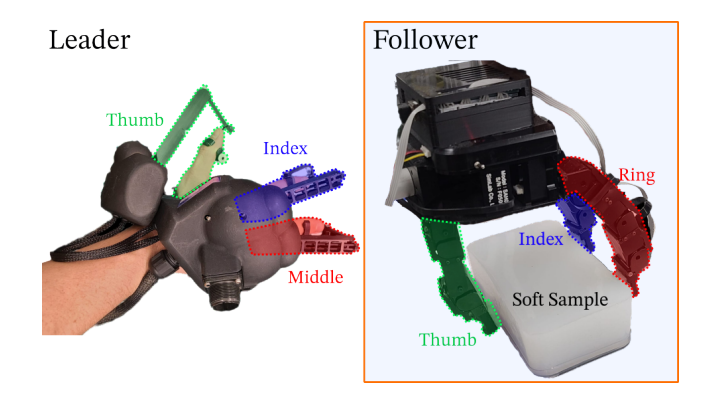


Fig. 1. Teleoperation setup connecting the Leader HGlove to the Allegro robotic hand. Forces measured from the robotic thumb, index, and ring fingers are rendered on the glove's thumb, index, and middle fingers, respectively. Departing from traditional camera-based approaches, our system is solely based on haptic feedback; the human users successfully accomplish the telemanipulation tasks without any visual input from the robot scene.

to control a remote robot (follower) receiving feedback from sensors placed on the remote robot or in the environment.

Vision is the dominant modality for sensing remote objects and environments, and visual feedback can easily be provided via monitors or Virtual Reality headsets. However, tactile and force sensing are valuable complementary modalities and often outperform vision in detecting vision in detecting physical properties such as stiffness. Haptic feedback devices that can effectively render these modalities are still uncommon [6].

Notably, although substantial research exists on autonomous robotic perception of stiffness using tactile sensing [7]–[9], object recognition via touch [10]–[12], and tactile assessment of specific object characteristics [13], there is little to no research on how human users with hand exoskeletons perceive object stiffness when relying solely on remote tactile sensing (follower) and kinesthetic haptic feedback (leader).

In this work, we address this gap by tasking ten participants with differentiating object stiffness using a bilateral telemanipulation system that provides kinesthetic haptic feedback. The setup is composed of an exoskeletal glove (HGlove [14]) on the leader side, which captures human hand and finger motion, thereby controlling the remote robot while also providing haptic feedback by applying kinesthetic forces onto the human fingers, and a dexterous robotic hand (Allegro Hand) equipped with tactile sensitive fingertips on the follower side, as shown in Fig. 1. Participants were required to squeeze five sample objects differing only in their level of stiffness (see Section IV-A) using the telemanipulation setup, and to then determine which of them is the most similar to a given

reference (**Task ABX**) and which of them is softer (**Task S**), as detailed in Section IV-D. We compare two methods of haptic feedback rendering: the first (see Section III-B1), which was initially introduced in [15], is based solely on the contact forces measured by the tactile sensors, while the second (newly proposed here, see Section III-B2) takes into consideration the squeeze displacement differences between the human and robot fingers, caused by kinematic mismatch between the leader and follower devices.

The main contributions of this work are:

- Demonstration of Stiffness Perception during Telemanipulation: Using a bilateral telemanipulation setup with haptic feedback on the leader and tactile sensing on the follower, we demonstrate that ten naive users can discriminate between five soft objects differing solely in stiffness by remotely squeezing them with a dexterous robotic hand while perceiving exclusively via haptic feedback (no visual cues), as shown in Fig. 3.
- Introduction of a novel Haptic Feedback method to perceive object stiffness: In Section III-B2, we introduce a novel method that incorporates finger displacement feedback in addition to force feedback, to address differences in the squeezing motion between the human operator and the robot caused by kinematic mismatches between the leader and follower devices a well established issue in telemanipulation.
- Insights from Statistical Analysis on User Preferences: Our analysis reveals that incorporating finger displacement feedback benefits naive users during more challenging tasks. While the advantage is not consistently significant across all conditions (see Tab. III), displacement feedback does enhance discrimination performance for objects of similar stiffness (as discussed in V-E).

#### II. RELATED WORKS

A wide range of studies has addressed automatic stiffness estimation or classification using tactile sensors [7], [9], [16], [17], as well as stiffness rendering through visual technologies [1], [18], [19]. However, fewer works have investigated stiffness rendering solely through haptic devices, we assume due to technological limitations. This study leverages data from haptic sensors in a telerobotic setup to identify a robust approach that enables operators to distinguish between soft objects during real-world teleoperation without visual feedback.

# A. Teleoperation

Telemanipulation is an extensive area with several comprehensive reviews meriting consideration [1], [5], [20]. The recent prominence of the field is illustrated by the ANA Avatar XPRIZE, a major non-medical teleoperation competition that challenges teams to develop systems excelling in intuitiveness, immersiveness, social interaction, robustness, and manipulation capacity across various tasks. Notable contributions have included the AvaTRINA Nursebot which combined haptic feedback with augmented reality [21], and the winning NimbRo Avatar system, which demonstrated robust telepresence and manipulation capabilities [22]. One entry [23] introduced

an exoskeletal glove for kinesthetic feedback, although this system provided limited force feedback during the competition, focusing principally on grasp detection rather than stiffness differentiation. Grasping force feedback has been studied by integrating tactile sensors with haptic devices, such as visuotactile sensing for dexterous manipulation [24] and vision-based tactile sensors for precise position-force teleoperation [25]. While these contributions have advanced telemanipulation technology, none have addressed stiffness perception or compared feedback methods.

# B. Stiffness Perception

To explore teleoperation systems that render stiffness information for soft objects, the field of telesurgery is particularly relevant. One study [26] demonstrated the value of haptic feedback in manipulating non-rigid objects. Recent advancements in surgical robotics have integrated haptic feedback to enhance real-time force reflection during procedures [6]. While systems like the da Vinci robot have lacked direct haptic feedback, studies using the da Vinci Research Kit (dVRK) have identified solutions [27], and the upcoming da Vinci 5 model will incorporate certified haptic feedback. The Senhance Surgical System also highlights the benefits of haptic feedback for precise control [6], while virtual simulations, such as those developed in [28], have provided realistic force feedback for training purposes. Additionally, haptic techniques using contact force control and virtual springs have been explored to improve transparency and stability [29], while other works [30] have focused on adaptive impedance control. Another work [31] explored the use of redundant haptic interfaces in teleoperated surgical systems to enhance soft-tissue stiffness discrimination by reducing apparent inertia and improving manipulability, leading to more accurate tissue stiffness perception during virtual palpation tasks. The advantages of cutaneous feedback in teleoperation, including improved stability and stiffness perception, have been demonstrated through shear force feedback [32] and enhanced dexterity via tactile cues such as friction feedback during in-hand manipulation [33].

The review in [34] has addressed soft tissue contact identification with a focus on visual stiffness maps obtained by palpation. Additionally, several studies have integrated medical instruments with industrial teleoperation systems. As an example, one study [35] used a teleoperation system with force feedback to evaluate users' ability to differentiate materials of varying stiffness during a palpation task. It combined a Haption Virtuose 6D haptic device as the leader and an industrial robot with a da Vinci Endowrist instrument as the follower. Our study, however, utilizes an exoskeleton glove offering haptic feedback perception directly onto the fingers, and is tested with more sample objects but without any visual feedback. Additionally, we compare two feedback methodologies to evaluate the respective roles of measured force and compression differences between the leader and follower.

# III. METHODOLOGY

## A. Teleoperation Setup

In this study, we utilize a portion of the robotic setup previously described in [15], [36]. Given our focus on the rendering of feedback forces on the fingers, we therefore limit the system to the Allegro robotic hand and the Leader HGlove exoskeleton as shown in Fig. 1. The HGlove provides two actuated degrees of freedom (DOFs) per finger for flexion and extension, delivering up to 5 N continuous force feedback, and one non-actuated DOF for lateral motion, which is left free but not used as a control command in this study. Each robotic finger of the follower hand is equipped with a magnetic tactile sensor based on the design in [37], consisting of four Halleffect units (MLX90393) in a 2×2 grid embedded in silicone [15]. Contact forces deform the silicone, displacing a 2 mm neodymium magnet and altering the magnetic field measured by the sensors. These variations, inspired by earlier designs [38]–[40], are sampled at 20 Hz to detect contact forces.

The sensors provide force measurements in three directions:  $F_x$ ,  $F_y$ , and  $F_z$ . In this study, we only use three fingers of the Allegro Hand  $j \in \{\text{thumb, index, ring}\}$ , to ensure a one-to-one correspondence with the fingers of the Leader HGlove  $i \in \{\text{thumb, index, middle}\}$ . This decision does not affect the setup's functionality but prevents potential errors due to interaction with the object at multiple closely spaced points. Transference of the measured forces runs in accordance with sensor-actuator haptic mapping as follows: thumb to thumb, index to index, and ring to middle.

The maximum force in the z-direction on the follower's side (subscript F) is defined as  $F_{F,j}$ :

$$F_{F,j} = \max(F_{z_1,j}, F_{z_2,j}, F_{z_3,j}, F_{z_4,j}) \tag{1}$$

The resulting force of each fingertip  $F_{{\rm F},j}$  can vary within a range of values greater than 0[digits]. However, for our purposes, we define a specific operational range for the force measurements using a minimum threshold  $F_{\rm F}^{\rm min}=30[digits]$  and a maximum threshold  $F_{\rm F}^{\rm max}=1000[digits]$ . Thus, the valid range for  $F_{{\rm F},j}$  is:

$$F_{\rm F}^{\rm min} \le F_{{\rm F},j} \le F_{\rm F}^{\rm max} \tag{2}$$

By incorporating these thresholds, we ensure that only meaningful force measurements within the specified range contribute to the feedback mechanisms, thereby enhancing the precision and reliability of the robotic finger's responses.

# B. Haptic Stiffness Feedback Methods

In this study, we test two methods for effective haptic feedback rendering, evaluating and characterizing the haptic experience when interacting with soft samples. The kinesthetic feedback is applied in joint space, as described in [15], to ensure precise rendering that aligns with the kinematics of the robotic hand and exoskeleton glove. For this purpose, we utilize the tactile information from the follower side,  $F_{{\rm F},j}$ , to generate two different haptic feedback methods on the leader side (subscript L), denoted as  $F_{L,j}^1$  and  $F_{L,j}^2$ . It is important to note that if the sensors are unable to record a contact force  $F_{{\rm F},j}$  above the minimum threshold, both methods would provide null haptic feedback. Thus:

$$\begin{cases} F_{L,j}^{1} = 0 \\ F_{L,j}^{2} = 0 \end{cases} \quad \text{if} \quad F_{F,j} < F_{F}^{\min}$$
 (3)

1) Method I: In this proposed method, the leader's feedback force  $F_{L,i}^1$  is rendered as:

$$F_{L,j}^1 = \alpha \cdot F_{F,j} \tag{4}$$

The constant scalar factor  $\alpha$  is defined as:

$$\alpha = \frac{F_{L,\text{max}}}{F_{\text{F}}^{\text{max}}} \tag{5}$$

where  $F_{L,\text{max}}$  represents the maximum force that the leader can apply, which is set to 5 N. This specification ensures that the maximum rendered force remains within the operational limits of the haptic glove, maintaining system integrity and functionality.

2) Method II: In this proposed method, the definition of the force rendered by the haptic glove  $F_{L,j}^2$  is based on real-time stiffness estimation through the tactile sensors. The stiffness of the measured samples can be defined as follows:

$$K_{F,j} = \frac{F_{F,j}}{\Delta Z_{F,j}} \tag{6}$$

where  $\Delta Z_{F,j}$  represents the displacement in the z-direction of the follower in response to a z-displacement  $\Delta Z_{L,j}$  of each leader's finger.

To relate the displacement of the robotic glove to the displacement of the robotic hand during contact, we define the parameter  $\Delta_Z$  as:

$$\Delta_Z = \frac{\Delta Z_{L,j}}{\Delta Z_{F,j}} \tag{7}$$

Additionally, we introduce the parameter  $\beta$ , defined as:

$$\beta = \frac{\Delta Z_{F,j}^{\text{max}}}{\Delta Z_{L,i}^{\text{max}}} \tag{8}$$

This parameter allows us to normalize the differences in movement between devices with different kinematic motion ranges. Consequently, the leader's feedback force  $F_{L,j}^2$  is given by:

$$F_{L,j}^2 = \alpha \cdot F_{F,j} \cdot \Delta_Z \cdot \beta = F_{L,j}^1 \cdot \Delta_Z \cdot \beta \tag{9}$$

# IV. EXPERIMENTS

# A. Object Description

In this study, each participant telemanipulated five soft samples of varying stiffness. These samples were made using ready-to-use commercial silicon mixes [Smooth-On, Inc. - USA], categorized according to their shore hardness (SH) [41], and labeled on the basis of their stiffness levels as follows (name of mix, SH):

- 1-US: Ultra-Soft (Ecoflex<sup>TM</sup> 00-10, SH: 00-10)
- 2-S: Soft (Ecoflex<sup>TM</sup> 00-30, SH: 00-30)
- 3-M: Medium (Ecoflex<sup>TM</sup> 00-50, SH: 00-50)
- 4-LH: Light-Hard (Dragon Skin<sup>TM</sup> 20, SH: A-20)
- 5-H: Hard (Dragon Skin<sup>TM</sup> 30, SH: A-30).

As shown in Fig. 2, these labels reflect the increasing stiffness of the samples, and provide a standardized measure to compare the haptic feedback experienced by the participants.

During the experiments, each sample was placed inside a small plastic container of the object mold's dimension fixed to the table to prevent unintended movement. The Allegro robotic hand squeezed the objects between its thumb and index and ring fingers, contacting the central top regions of the opposing lateral faces of the sample, as shown in Fig. 1. The setting guaranteed that the robotic fingers did not interact with the table or container during squeezing, eliminating confounding factors in force-feedback measurements.

# B. Participants Preparation

The experimental procedure began by adjusting the chair to ensure participant comfort and accessibility. The study involved ten right-handed participants aged 20 to 35 years, without prior physical problems. Participants completed a consent form detailing the feedback method used during the experiment, and a further form in which they acknowledged and approved the conditions and ethics that belay the experiments. They then put on the HGlove and received instructions on how to reattach it if it became dislodged, as this would require the trial to be repeated. Participants were instructed to move their fingers slowly and in a controlled manner to prevent delays and avoid reflex forces.

# C. Training Session

A five-minute training session was conducted, in which participants teleoperated the Allegro robotic hand to squeeze an object (sample 3-M) for 90 seconds while visually observing the interaction. Following this, participants squeezed three different samples in a known predefined sequence (sample 1-US, sample 3-M, sample 5-H) for 30 seconds each. Subsequently, a panel was put in place to prevent participants from seeing the robot and sample objects.

# D. Tasks

The first task was of type  $\mathbf{ABX}$  [42]. During this task, participants were presented with two objects (A and B) for 10 seconds each, followed by a third object (X). They were then asked to determine whether X was more similar to A or to B. We refer to this task as  $\mathbf{Task}$   $\mathbf{ABX}$ .

In the second task participants were asked to answer the following question, "Which object, out of A and B is softer?". We refer to this task as **Task S**.

To familiarize participants with the tasks, two practice trials were undertaken at the beginning of the session, using the following sample sequences: [1 - US, 3 - M, 1 - US] and [5 - H, 3 - M, 3 - M]. These results were not recorded.

#### E. Experimental Design

The experimental session consisted of 24 **Task ABX** tests and 24 **Task S** tests, each conducted in three blocks of eight. The sequence of experiments presented to each participant in both methods is detailed in Table II. As illustrated, sequences [1-8] are identical to sequences [17-24], while in sequences [9-16], the values of A and B were inverted, with X remaining unchanged. The values of X were selected to represent

extreme and medium stiffness levels - specifically X=1-US, X=3-M, and X=5-H.

We designed the trials to evaluate four levels of perceptual distance (D=1,2,3,4), each defined by the difference in stiffness levels between stimuli. Each distance level was represented by two distinct pairs of stimuli, and each distance level appeared six times in the experimental session, ensuring balanced representation across all levels. As each of the eight pairs was tested three times, this also ensured a balanced distribution of trials among the pairs. The specific pairs for each distance level are reported in Table I.

TABLE I PAIRS AND DISTANCES FOR THE EXPERIMENT

Distance (D)	A	В	X
1	1-US	2-S	1-US
1	3-M	4-LH	3-M
2	1-US	3-M	3-M
2	3-M	5-H	5-H
3	1-US	4-LH	1-US
3	2-S	5-H	5-H
4	1-US	5-H	1-US
4	5-H	1-US	5-H

In Table II, the distance D and the direction of difference are both reported; an upward arrow (↑) indicates that the object deemed less similar to X is harder than X, while a downward arrow (1) indicates that it is softer. Participants were unaware that the sequences across the two days were the same, having been informed that the sequences were randomly generated. After each set of eight experiments, participants were given a 60-second break during which the glove was readjusted if necessary. Stimuli within each trial were presented in a randomized order to mitigate sequence effects and potential biases. The assignment of the X stimulus (the target) to match either stimulus A or B was also randomized across trials. This approach aligns with a key requirement of the ABX test, which stipulates that multiple trials must be performed to make statistically confident assertions about a participant's ability to distinguish between stimuli [43]. Additionally, limiting the session to 24 trials adheres to guidelines aimed at preventing participant fatigue, thereby maintaining the sensitivity and reliability of the test results.

Two kinesthetic haptic feedback methods were employed: Method I and Method II. Each participant completed two sessions, alternating between the feedback methods. To mitigate any potential bias related to the learning curve, half of the participants started the first session with Method I, while the other half began with Method II. Each experimental session lasted approximately 40 to 45 minutes, including about 10 minutes for setup, training and rest, and approximately 30 minutes dedicated to the experiments.

# V. DATA ANALYSIS AND RESULTS

## A. Statistical Confidence Level

In the ABX test, each trial has a 50% chance of a correct response under the null hypothesis of random guessing. Using the binomial distribution with n=24 trials and success probability p=0.5, the probability of obtaining at least 16 correct responses by chance (66.66% of success rate) is approximately 10.6%:

$$P(X \ge 16) = \sum_{k=16}^{24} {24 \choose k} (0.5)^{24} \approx 10.6\%.$$
 (10)

This corresponds to a confidence level of approximately 89.4%. While this does not meet the threshold for statistical significance at the 90% confidence level, it suggests a trend toward significance in participants' ability to discriminate between stimuli.

To achieve statistical significance above the 95% confidence level, participants need, on average, at least 17 correct responses (70.8% of success rate), as the probability of obtaining this result by chance is approximately 4.3%:

$$P(X \ge 17) \approx 4.3\%.$$
 (11)

On that basis we can reject the null hypothesis at the 95% confidence level, indicating a statistically significant ability to discriminate between stimuli.



Fig. 2. Soft material samples composed of gel or silicone, numbered from 1 to 5 in increasing stiffness. E: Ecoflex<sup>TM</sup> 00-10, 00-30, 00-50; DS: Dragon Skin<sup>TM</sup> A-20, A-30. This figure has been edited for clarity.

# B. Overall Performance Comparison

The box plot in Fig. 3 depicts the overall performance of the participants for **Task ABX** and **Task S** using the two methods, regardless of the day of the experimental session.

- Task ABX Performance: Both methods exhibit relatively high success rates for Task ABX, with mean success rates around 75%. However, Method II shows lower variability, indicating more consistent performance by participants, as evidenced by lower variance and standard deviation.
- Task S Performance: Here again, we find similar success rates. Method I results show a slightly higher median success rate (67.91%) than Method II (64.58%). However, with Method II we see a broader spread in performance, indicating greater variability among participants. The presence of potential outliers suggests that some participants faced difficulties with Method II in Task S.

The box plot in Fig. 3 shows that for **Task ABX**, Method II guarantees higher performance consistency. For **Task S**, while Method I results in a slightly higher median, Method II scores exhibit greater variability, indicating that individual differences or task-specific challenges are more pronounced using this method.

# C. Daily Performance Comparison

One limitation of the previous analysis is the potential learning effect between Day 1 and Day 2. To address this, we separated the participants into two groups:

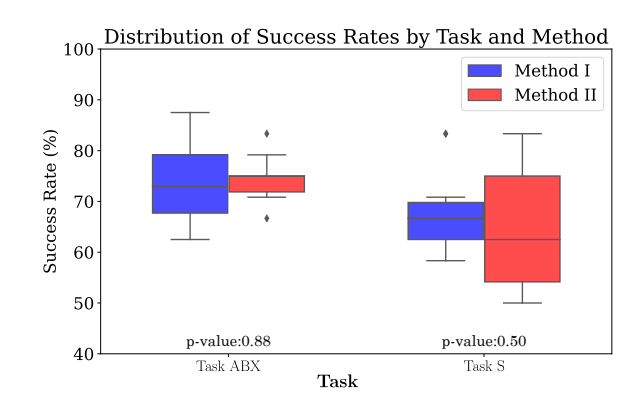


Fig. 3. The graph compares the overall success rate for each task by method, with Task ABX results on the left and Task S results on the right, without differentiating between experimental days. ♦ are the outliers.

- **Group 1**: Participants who started with Method I (blue) on Day 1 and continued with Method II (red) on Day 2.
- **Group 2**: Participants who started with Method II on Day 1 and continued with Method I on Day 2.

The bar plot in Fig. 4 illustrates the success rates of the two groups across the two tasks (**ABX** and **S**) with distinct methods applied on different days. Each bar represents the mean success rate for a specific group on a specific day and task. The graph reveals several key observations:

- Both groups show an average improvement in performance between the first and second day of testing for each task. Group 1 improved in **Task ABX** from 69.16% to 75%, an increase of approximately 6.0% (p = 0.021, statistically significant), and in **Task S** from 68.33% to 73.33%, an increase of approximately 5.0% (p = 0.235, not statistically significant). Group 2 also shows an improvement from 74.17% to 79.17% between the first and second day on **Task ABX** (p = 0.063, marginally significant) and a noticeable improvement in **Task S** from 55.83% to 67.50%, an increase of approximately 11.7% (p = 0.039, statistically significant).
- Group 1 exhibited similar performance across both tasks, with statistically significant improvement only in Task ABX. In contrast, Group 2 outperformed Group 1 in Task ABX but showed generally lower performance in Task S, despite achieving statistically significant improvement on this task between Day 1 and Day 2.

# D. Analysis of Variance (ANOVA)

A two-way ANOVA was conducted to examine the effects of *Group*, *Day*, and *Task* on the mean *Success Rate*, along with their interaction effects. The analysis tested the following main effects and interactions:

- **Group**: Evaluating the influence of participant group on success rates.
- Day: Assessing the impact of the day on which the task was performed on success rates.
- Task: Determining the effect of the type of task on success rates.
- Interactions: Investigating interactions between Group and Day, Group and Task, and Day and Task.

#### TABLE II SEQUENCE OF ABX TESTS

Test	1	2	3	4	5	6	7	8	9	10	11	12	13	14	15	16	17	18	19	20	21	22	23	24
A	1	2	4	3	5	2	1	3	5	5	3	1	1	1	4	5	1	2	4	3	5	2	1	3
В	5	5	3	1	1	1	4	5	1	2	4	3	5	2	1	3	5	5	3	1	1	1	4	5
X	1	5	3	3	5	1	1	5	1	5	3	3	5	1	1	5	1	5	3	3	5	1	1	5
D	4	3	1	2	4	1	3	2	4	3	1	2	4	1	3	2	4	3	1	2	4	1	3	2
	↑	↓	1	↓	↓	1	1	↓	1	↓	↑	↓	↓	↑	↑	↓	1	↓	↑	↓	↓	↑	↑	↓

TABLE III MEAN SUCCESS RATES, VARIANCES, AND STANDARD DEVIATIONS FOR TASKS X AND S BY METHOD

Task	Method	Mean Success Rate (%)	Std Deviation		
ABX	1	74.16	64.83	8.05	
ABX	2	74.58	21.04	4.59	
S	1	67.91	81.20	9.01	
S	2	64.58	159.14	12.62	

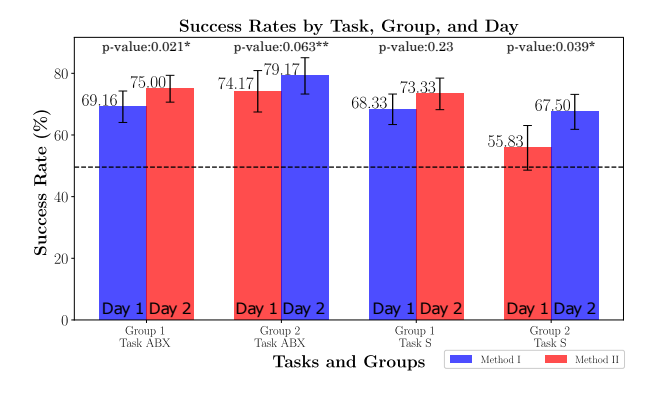


Fig. 4. Task success rates for both groups, subdivided by experimental days and methods applied. The p-values are annotated on the plot, with an asterisk (\*) indicating statistically significant results and a double asterisk (\*\*) denoting marginally significant results.

The results of the ANOVA are presented in Table IV and the results are summarized as follows:

Source	Sum of Squares	df	F-Statistic	p-value
Group	10.47	1	1.48	0.437
Day	94.60	1	13.42	0.170
Task	132.11	1	18.74	0.145
Group:Day	4.25	1	0.60	0.580
Group:Task	94.60	1	13.42	0.170
Day:Task	4.25	1	0.60	0.580
Residual	7.05	1	-	-

- The effect of **Group** on the *Success Rate* was not statistically significant,  $F=1.48,\ p=0.437,$  indicating that group assignment did not significantly influence participants' success rates.
- The effect of **Day** on the *Success Rate* was also not statistically significant, F=13.42, p=0.170, suggesting that the day of task performance did not significantly affect success rates.
- The effect of **Task** on the *Success Rate* was not statistically significant, F=18.74, p=0.145, implying that the success rates did not differ significantly between tasks.
- The interactions between **Group** and **Day** (F = 0.60, p = 0.580), **Group** and **Task** (F = 13.42, p = 0.170),

and **Day** and **Task** (F = 0.60, p = 0.580) were all not statistically significant.

The ANOVA results indicate no statistically significant differences in success rates across groups, days, or tasks. Additionally, the lack of significant interaction effects suggests that the combination of these factors did not meaningfully influence outcomes. Thus, variations in success rates cannot be attributed to participant grouping or task types. The relatively high F-values observed for factors such as *Day* and *Task*, paired with non-significant p-values, suggest that while some differences exist, they are not substantial enough to achieve statistical significance. The residual sum of squares (7.05) indicates that a significant portion of the variability in success rates remains unexplained by the factors of Group, Day, Task, or their interactions.

# E. Performance and Statistical Analysis Across Sample Pairs

As presented in Section IV-A, the samples used during the experiments are classified into seven different pairs, which are further grouped according to their differences in stiffness (denoted as **D** as shown in Table II).

To assess suitability for parametric testing, we first evaluated normality and homogeneity of variances in success rates for each object pair and each method using the Shapiro-Wilk and Levene's tests, respectively. The Shapiro-Wilk results indicated significant deviations from normality (p < 0.05) in most groups, while Levene's test showed inconsistent homogeneity across pairs and tasks, suggesting that parametric assumptions were not met.

Given these results, we employed the Mann-Whitney U test (MWU), a non-parametric alternative to the t-test, to compare success rates between Method I and Method II for each object pair and task (ABX and S). This test ranks observations across both methods and calculates the U statistic, indicating the extent of difference in rank distributions between the methods. With statistical significance set at p < 0.05, in only one pairing (1-US, 4-LH) in **Task S** did we see a significant difference between the methods (p = 0.048). For all other pairings, the analysis showed p > 0.05, indicating comparable success rates between the methods across pairs and tasks. To visualize these findings, we generated spider plots, shown in Fig. 5 and Fig. 6, which depict success rates across object pairs for each method.

To further explore these differences, we aggregated object pairs by stiffness distance into three groups:  $\mathbf{D}=\mathbf{1},\,\mathbf{D}=\mathbf{2},\,$  and  $\mathbf{D}=\mathbf{3}.$  The MWU test was applied to each distance group independently for both ABX and S tasks. Although no group reached p<0.05 significance, results for the ABX task produced p-values close to this threshold,  $\mathbf{D}=\mathbf{1}$  (p=0.061) and  $\mathbf{D}=\mathbf{3}$  (p=0.067), suggesting a potential trend towards

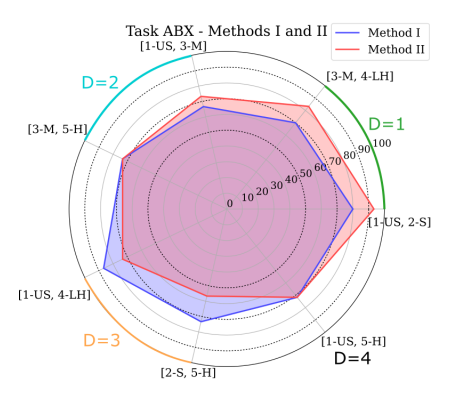


Fig. 5. Spider plot showing Success Rate performance for Methods I and II in Task ABX for object pairs.

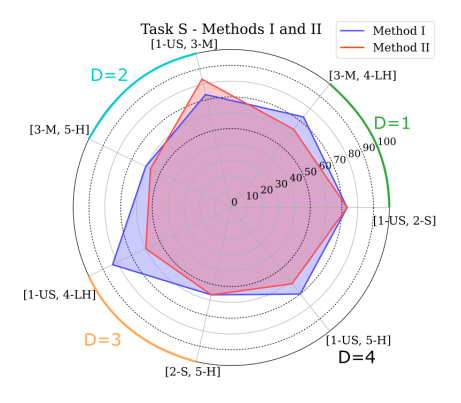


Fig. 6. Spider plot showing Success Rate performance for Methods I and II in Task S for object pairs.

significance. In light of these findings, we computed mean success rates for Method I and Method II within each distance group to better understand performance patterns. For the ABX task, Method II showed higher mean success rates than Method I for  $\mathbf{D} = \mathbf{1}$  (88% vs. 75%), while Method I outperformed Method II for  $\mathbf{D} = \mathbf{3}$  (80% vs. 65%). In the S task, Method I consistently led to higher mean success rates for both  $\mathbf{D} = \mathbf{1}$  (73% vs. 68%) and  $\mathbf{D} = \mathbf{3}$  (65% vs. 58%).

#### VI. DISCUSSION

Task ABX revealed distinct performance trends between feedback methods - using Method II led to higher success rates for smaller stiffness differences (**D=1**), while Method I led to higher success rates for larger contrasts (D=3), as evidenced by the spider plots in Fig. 5. This suggests that in more complex tasks (i.e. smaller stiffness differences) the addition of a kinematic component to the force feedback (i.e. Method II) improves discrimination performances, while this effect is not evident for easier tasks (i.e. larger stiffness differences), in which a simpler method based on force feedback only (i.e. Method I) leads to better performance. In Task S, the two methods exhibited comparable performance, albeit with lower overall success rates, though Method I showed a statistically significant advantage for one pair (1-US, 4-LH). These results align with the spider plots in Fig. 6, which highlight reduced perceptual discriminability in direct softness comparisons as opposed to similarity discrimination tasks. Additionally, as shown in Fig. 4, in the case of **Task ABX**, both groups demonstrated a statistically significant improvement in task performance between Day 1 and Day 2. For **Task S**, an observable improvement was significant only for Group 2 making it challenging to draw definitive conclusions about the learning effects for this task.

Some observations warrant deeper discussion. Although it might be expected that materials with greater differences in softness would yield near-perfect scores, this was not consistently observed. For example, D=3 comparisons outperformed D=4 when paired with 1-US. While no statistical significance was found, the spider plots indicate that tests involving the hardest object (5-H) tend to yield poorer results. This may be due to force saturation, as the maximum force threshold of 5 N compresses the dynamic range of feedback and limits perceptual differentiation. Additionally, material hysteresis in harder silicone samples could alter tactile cues during compression, reducing consistency in perceived stiffness. Another plausible explanation relates to the optimal sensitivity range of human tactile perception; intermediate stiffness differences (D = 3) may fall within a range within which discriminability peaks, whereas extreme contrasts (D = 4) may exceed this range and introduce perceptual challenges.

# VII. CONCLUSIONS

This study tested two methodologies for rendering haptic stiffness feedback during robotic telemanipulation. The first methodology, Method I, provided haptic feedback proportional solely to the contact forces measured by tactile sensors on the robotic hand. The second methodology, Method II, augmented this feedback by incorporating finger displacement during object squeezing to compensate for the kinematic mismatch between the exoskeleton glove and the robotic hand. Both methodologies were tested in a bilateral teleoperation setup in which participants squeezed soft objects to discriminate their stiffness without visual cues. For Task ABX, in which participants had to identify which object was most similar to a reference, the average success rate was approximately 75% for both methods, exceeding the 95% confidence threshold. For **Task S**, in which participants had to determine which object was softer, success rates averaged around 65%, approaching the 90% confidence threshold. Overall, these findings confirm that haptic feedback alone can indeed support effective stiffness discrimination during telemanipulation tasks.

#### REFERENCES

- [1] Y. Deng, Y. Tang, B. Yang, W. Zheng, S. Liu, and C. Liu, "A review of bilateral teleoperation control strategies with soft environment," in 2021 6th IEEE International Conference on Advanced Robotics and Mechatronics (ICARM). IEEE, 2021, pp. 459–464.
- [2] D. Zhang, W. Si, W. Fan, Y. Guan, and C. Yang, "From teleoperation to autonomous robot-assisted microsurgery: A survey," *Machine Intelli*gence Research, vol. 19, no. 4, pp. 288–306, 2022.
- [3] S. N. F. Nahri, S. Du, and B. J. Van Wyk, "A review on haptic bilateral teleoperation systems," *Journal of Intelligent & Robotic Systems*, vol. 104, no. 1, p. 13, 2022.
- [4] I. Vitanov, I. Farkhatdinov, B. Denoun, F. Palermo, A. Otaran, J. Brown, B. Omarali, T. Abrar, M. Hansard, C. Oh *et al.*, "A suite of robotic solutions for nuclear waste decommissioning," *Robotics*, vol. 10, no. 4, p. 112, 2021.

- [5] K. Darvish, L. Penco, J. Ramos, R. Cisneros, J. Pratt, E. Yoshida, S. Ivaldi, and D. Pucci, "Teleoperation of humanoid robots: A survey," *IEEE Transactions on Robotics*, vol. 39, no. 3, pp. 1706–1727, 2023.
- [6] R. V. Patel, S. F. Atashzar, and M. Tavakoli, "Haptic feedback and force-based teleoperation in surgical robotics," *Proceedings of the IEEE*, vol. 110, no. 7, pp. 1012–1027, 2022.
- [7] Q. Li, O. Kroemer, Z. Su, F. F. Veiga, M. Kaboli, and H. J. Ritter, "A review of tactile information: Perception and action through touch," *IEEE Transactions on Robotics*, vol. 36, no. 6, pp. 1619–1634, 2020.
- [8] M. Bednarek, P. Kicki, J. Bednarek, and K. Walas, "Gaining a sense of touch object stiffness estimation using a soft gripper and neural networks," *Electronics*, vol. 10, no. 1, 2021.
- [9] J. Huang and A. Rosendo, "Variable stiffness object recognition with a cnn-bayes classifier on a soft gripper," *Soft Robotics*, vol. 9, no. 6, pp. 1220–1231, 2022.
- [10] H. Liu, Y. Wu, F. Sun, and D. Guo, "Recent progress on tactile object recognition," *International Journal of Advanced Robotic Systems*, vol. 14, no. 4, 2017.
- [11] E. Kirby, R. Zenha, and L. Jamone, "Comparing single touch to dynamic exploratory procedures for robotic tactile object recognition," *IEEE Robotics and Automation Letters*, vol. 7, no. 2, pp. 4252–4258, 2022.
- [12] S. Funabashi, G. Yan, F. Hongyi, A. Schmitz, L. Jamone, T. Ogata, and S. Sugano, "Tactile transfer learning and object recognition with a multifingered hand using morphology specific convolutional neural networks," *IEEE Transactions on Neural Networks and Learning Systems*, vol. 35, no. 6, pp. 7587–7601, 2024.
- [13] P. Ribeiro, S. Cardoso, A. Bernardino, and L. Jamone, "Fruit quality control by surface analysis using a bio-inspired soft tactile sensor," in 2020 IEEE/RSJ International Conference on Intelligent Robots and Systems (IROS), 2020, pp. 8875–8881.
- [14] J. Perret, Q. Parent, and B. Giudicelli, "Hglove: A wearable force-feedback device for the hand," in 14th annual EuroVR conference, 2017.
- [15] G. Giudici, B. Omarali, A. A. Bonzini, K. Althoefer, I. Farkhatdinov, and L. Jamone, "Feeling good: Validation of bilateral tactile telemanipulation for a dexterous robot," in *Annual Conference Towards Autonomous Robotic Systems*. Springer, 2023, pp. 443–454.
- [16] N. Mavrakis and R. Stolkin, "Estimation and exploitation of objects' inertial parameters in robotic grasping and manipulation: A survey," *Robotics and Autonomous Systems*, vol. 124, p. 103374, 2020.
- [17] B. Omarali, F. Palermo, K. Althoefer, M. Valle, and I. Farkhatdinov, "Tactile classification of object materials for virtual reality based robot teleoperation," in 2022 International Conference on Robotics and Automation (ICRA). IEEE, 2022, pp. 9288–9294.
- [18] T. Yamamoto, B. Vagvolgyi, K. Balaji, L. L. Whitcomb, and A. M. Okamura, "Tissue property estimation and graphical display for teleoperated robot-assisted surgery," in 2009 IEEE International Conference on Robotics and Automation. IEEE, 2009, pp. 4239–4245.
- [19] G. Meccariello, F. Faedi, S. AlGhamdi, F. Montevecchi, E. Firinu, C. Zanotti, D. Cavaliere, R. Gunelli, M. Taurchini, A. Amadori et al., "An experimental study about haptic feedback in robotic surgery: may visual feedback substitute tactile feedback?" *Journal of robotic surgery*, vol. 10, pp. 57–61, 2016.
- [20] M. Suomalainen, Y. Karayiannidis, and V. Kyrki, "A survey of robot manipulation in contact," *Robotics and Autonomous Systems*, vol. 156, p. 104224, 2022.
- [21] J. M. Marques, J.-C. Peng, P. Naughton, Y. Zhu, J. S. Nam, and K. Hauser, "Commodity telepresence with team avatrina's nursebot in the ana avatar xprize finals," in *Proc. 2nd Workshop Toward Robot Avatars IEEE Int. Conf. Robot. Autom.(ICRA)*, 2023, pp. 1–3.
- [22] M. Schwarz, C. Lenz, R. Memmesheimer, B. Pätzold, A. Rochow, M. Schreiber, and S. Behnke, "Robust immersive telepresence and mobile telemanipulation: Nimbro wins ana avatar xprize finals," in 2023 IEEE-RAS 22nd International Conference on Humanoid Robots (Humanoids). IEEE, 2023, pp. 1–8.
- [23] B. Park, D. Kim, D. Lim, S. Park, J. Ahn, S. Kim, J. Shin, E. Sung, J. Sim, J. Kim et al., "Intuitive and interactive robotic avatar system for tele-existence: Team snu in the ana avatar xprize finals," *International Journal of Social Robotics*, pp. 1–29, 2024.
- [24] N. Becker, K. Sovailo, C. Zhu, E. Gattung, K. Hansel, T. Schneider, Y. Zhu, Y. Hasegawa, and J. Peters, "Integrating and evaluating visuotactile sensing with haptic feedback for teleoperated robot manipulation," arXiv preprint arXiv:2404.19585, 2024.
- [25] Y. Zhu, S. Nazirjonov, B. Jiang, J. Colan, T. Aoyama, Y. Hasegawa, B. Belousov, K. Hansel, and J. Peters, "Visual tactile sensor based force estimation for position-force teleoperation," in 2022 IEEE International Conference on Cyborg and Bionic Systems (CBS). IEEE, 2023, pp. 49–52.

- [26] F. Danion, J. S. Diamond, and J. R. Flanagan, "The role of haptic feed-back when manipulating nonrigid objects," *Journal of neurophysiology*, vol. 107, no. 1, pp. 433–441, 2012.
- [27] C. D'Ettorre, A. Mariani, A. Stilli, F. R. y Baena, P. Valdastri, A. Deguet, P. Kazanzides, R. H. Taylor, G. S. Fischer, S. P. DiMaio et al., "Accelerating surgical robotics research: A review of 10 years with the da vinci research kit," *IEEE Robotics & Automation Magazine*, vol. 28, no. 4, pp. 56–78, 2021.
- [28] Y. Kuroda, M. Nakao, T. Kuroda, H. Oyama, and M. Komori, "Interaction model between elastic objects for haptic feedback considering collisions of soft tissue," *Computer Methods and Programs in Biomedicine*, vol. 80, no. 3, pp. 216–224, 2005.
- [29] J. Park and O. Khatib, "A haptic teleoperation approach based on contact force control," *The International Journal of Robotics Research*, vol. 25, no. 5-6, pp. 575–591, 2006.
- [30] S. V. Velanas and C. S. Tzafestas, "Human telehaptic perception of stiffness using an adaptive impedance reflection bilateral teleoperation control scheme," in 19th International Symposium in Robot and Human Interactive Communication. IEEE, 2010, pp. 21–26.
- [31] A. Torabi, M. Khadem, K. Zareinia, G. R. Sutherland, and M. Tavakoli, "Application of a redundant haptic interface in enhancing soft-tissue stiffness discrimination," *IEEE Robotics and Automation Letters*, vol. 4, no. 2, pp. 1037–1044, 2019.
- [32] C. Pacchierotti, A. Tirmizi, G. Bianchini, and D. Prattichizzo, "Enhancing the performance of passive teleoperation systems via cutaneous feedback," *IEEE transactions on haptics*, vol. 8, no. 4, pp. 397–409, 2015
- [33] Y. Zhu, J. Colan, T. Aoyama, and Y. Hasegawa, "Cutaneous feedback interface for teleoperated in-hand manipulation," in 2022 IEEE/RSJ International Conference on Intelligent Robots and Systems (IROS). IEEE, 2022, pp. 605–611.
- [34] T. D. Nagy and T. Haidegger, "Recent advances in robot-assisted surgery: Soft tissue contact identification," in 2019 IEEE 13th International Symposium on Applied Computational Intelligence and Informatics (SACI). IEEE, 2019, pp. 99–106.
- [35] E. Psomopoulou, R. Persad, A. Koupparis, S. Abeywardena, M. F. Sani, C. Melhuish, and S. Dogramadzi, "Evaluation of force feedback for palpation and application of active constraints on a teleoperated system," in *Proceedings of MEDICON 2019, September 26-28, 2019, Coimbra, Portugal.* Springer, 2020, pp. 1571–1580.
- [36] X. Mao, G. Giudici, C. Coppola, K. Althoefer, I. Farkhatdinov, Z. Li, and L. Jamone, "Dexskills: Skill segmentation using haptic data for learning autonomous long-horizon robotic manipulation tasks," in 2024 IEEE/RSJ International Conference on Intelligent Robots and Systems (IROS). IEEE, 2024, pp. 5104–5111.
- [37] A. A. Bonzini, L. Seminara, S. Macciò, A. Carfi, and L. Jamone, "Leveraging symmetry detection to speed up haptic object exploration in robots," in 2022 IEEE International Conference on Development and Learning (ICDL). IEEE, 2022, pp. 95–100.
- [38] T. P. Tomo, S. Somlor, A. Schmitz, S. Hashimoto, S. Sugano, and L. Jamone, "Development of a hall-effect based skin sensor," in 2015 IEEE SENSORS. IEEE, 2015, pp. 1–4.
- [39] T. Paulino, P. Ribeiro, M. Neto, S. Cardoso, A. Schmitz, J. Santos-Victor, A. Bernardino, and L. Jamone, "Low-cost 3-axis soft tactile sensors for the human-friendly robot vizzy," in 2017 IEEE international conference on robotics and automation (ICRA). IEEE, 2017, pp. 966–971.
- [40] T. P. Tomo, A. Schmitz, W. K. Wong, H. Kristanto, S. Somlor, J. Hwang, L. Jamone, and S. Sugano, "Covering a robot fingertip with uskin: A soft electronic skin with distributed 3-axis force sensitive elements for robot hands," *IEEE Robotics and Automation Letters*, vol. 3, no. 1, pp. 124–131, 2017.
- [41] H. Qi, K. Joyce, and M. Boyce, "Durometer hardness and the stress-strain behavior of elastomeric materials," *Rubber chemistry and technology*, vol. 76, no. 2, pp. 419–435, 2003.
- [42] W. Munson and M. B. Gardner, "Standardizing auditory tests," The Journal of the Acoustical Society of America, vol. 22, no. 5\_Supplement, pp. 675–675, 1950.
- [43] R. E. Greenaway, "Abx discrimination task," in *Discrimination testing in sensory science*. Elsevier, 2017, pp. 267–288.